

# Polarization entangled state measurement on a chip

Linda Sansoni,<sup>1</sup> Fabio Sciarrino,<sup>1,2</sup> Giuseppe Vallone,<sup>3,1</sup> Paolo Mataloni,<sup>1,2</sup>  
Andrea Crespi,<sup>4,5</sup> Roberta Ramponi,<sup>4,5</sup> and Roberto Osellame<sup>4,5</sup>

<sup>1</sup>*Dipartimento di Fisica, Sapienza Università di Roma, I-00185 Roma, Italy*

<sup>2</sup>*Istituto Nazionale di Ottica, Consiglio Nazionale delle Ricerche (INO-CNR), L.go E. Fermi 6, I-50125 Firenze, Italy*

<sup>3</sup>*Museo Storico della Fisica e Centro Studi e Ricerche Enrico Fermi,  
Via Panisperna 89/A, Compendio del Viminale, I-00184 Roma, Italy*

<sup>4</sup>*Istituto di Fotonica e Nanotecnologie, Consiglio Nazionale delle  
Ricerche (IFN-CNR), Piazza L. da Vinci, 32, I-20133 Milano, Italy*

<sup>5</sup>*Dipartimento di Fisica, Politecnico di Milano, Piazza L. da Vinci, 32, I-20133 Milano, Italy*

The emerging strategy to overcome the limitations of bulk quantum optics consists of taking advantage of the robustness and compactness achievable by the integrated waveguide technology. Here we report the realization of a directional coupler, fabricated by femtosecond laser waveguide writing, acting as an integrated beam splitter able to support polarization encoded qubits. This maskless and single step technique allows to realize circular transverse waveguide profiles able to support the propagation of Gaussian modes with any polarization state. Using this device, we demonstrate the quantum interference with polarization entangled states and singlet state projection.

Photons are the natural candidate for Quantum Information (QI) transmission [1, 2], quantum computing [3, 4] optical quantum sensing and metrology [5]. However, the current optical technology does not allow the transition to ultimate applications for many practical limitations. Complex quantum optical schemes, realized in bulk optics suffers from severe limitations, as far as stability, precision and physical size are concerned. Indeed, it is a difficult task to build advanced interferometric structure using bulk-optical components with the stability and the optical phase control accuracy necessary to reach the sensitivity allowed by quantum mechanics. Furthermore, it is very difficult to reach this task outside environments with controlled temperature and vibrations, and this makes applications outside laboratory hard to achieve.

The present approach to beat these limitations is to adopt miniaturized optical waveguide devices. Very recently it was reported [6, 7] that silica waveguide circuits integrated onto silicon chips can be successfully used to realize key components of quantum photonic devices. Inherently stable interferometers were shown to demonstrate phase stability, not only of single path encoded qubits, but also of two-photon entangled Fock state. On this basis, miniaturized integrated quantum circuits were realized to implement the first integrated linear optical control-NOT gate, achieving a fidelity very close to the theoretical value [6]. More recently, novel components for adaptive quantum circuits have also been demonstrated [8]. These experiments demonstrate robust and accurate phase control in integrated, path-encoded waveguide systems. Similar results have been obtained in UV laser written optical circuits fabricated in a suitable stack of doped silica layers on a silicon substrate [9].

All the experiments performed so far with integrated quantum circuits are based only on path encoded qubits with a given polarization state of the photons. On the

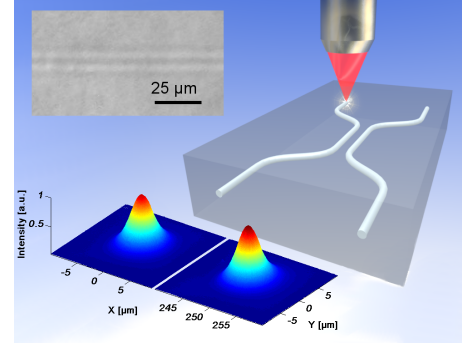


FIG. 1: Schematic of the femtosecond-laser-written directional coupler in the bulk of a borosilicate glass. Upper inset shows a microscope image of the two waveguides in the coupling region. Lower inset shows the near-field intensity profile of the output guided modes of the directional coupler by launching light in a single input; the symmetric Gaussian shape and the balanced splitting in the two arms can be appreciated.

other hand, many QI processes and sources of entangled photon states are based on the polarization degree of freedom [4]. One important example is given by states built on many photons [10] and/or many qubits, and by several schemes of one-way optical quantum computing [11]. Hence it is of essential interest to include the use of photon polarization in quantum circuits by fabricating integrated polarization independent devices, i.e. able to efficiently guide and manipulate photons in any polarization state.

It has to be noticed that the above mentioned silica-on-silicon and UV written integrated waveguides suffer from intrinsic birefringence (usually reported in the order of  $4 \times 10^{-4}$  [12, 13]). In fact, these waveguides are fabricated in a doped silica multilayer structure on a silicon substrate and this causes material stress due to lattice

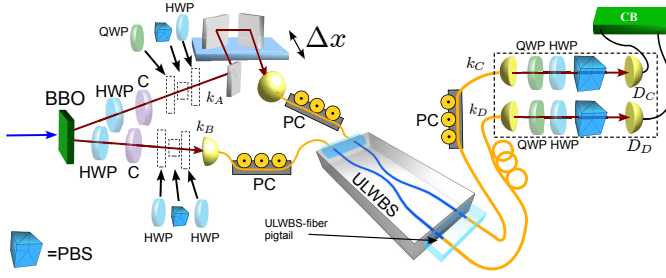


FIG. 2: Setup for the quantum optics experiments showing the source of polarization-entangled photons, the ULWBS and the detection system. Polarizing beam splitter (PBS), half (HWP) and quarter (QWP) waveplates were optionally inserted in path  $k_A$  and  $k_B$  to prepare different input states. A delay line  $\Delta x$  in the  $k_A$  arm enabled temporal delay variation between the two input photons. The components shown in the dashed box were inserted only during the tomography measurement of the filtered state. C: crystal compensators, PC: polarization controllers.

mismatches between the different layers. Techniques for reducing this stress and the induced birefringence have been proposed, but they pose serious difficulties in terms of fabrication complexity and reproducibility [14]. Such birefringence causes polarization-mode dispersion and results in polarization dependent behavior of the integrated devices, which removes indistinguishability between the two polarizations. Moreover, propagation in birefringent structures can cause decoherence of large-bandwidth (short coherence time) photons typically generated in parametric down-conversion experiments. As a consequence, the techniques already employed for producing path-encoded quantum circuits are not appropriate for processing polarization-encoded qubits in integrated devices.

In the present paper we show how to guide and manipulate photons in any polarization state by adopting a recently introduced technique, based on the use of ultrashort laser pulses, for direct writing of photonic structures in a bulk glass [15, 16]. Precisely, here, for the first time, we demonstrate the maintenance of polarization entanglement and Bell-state analysis in an integrated symmetric (50/50) beam splitter, opening the way to the use of polarization entanglement in integrated circuits for QI processes.

Direct fabrication of buried waveguides in glass is obtained by femtosecond laser micromachining. Femtosecond infrared pulses, focused into the substrate using a microscope objective, induce non-linear absorption phenomena based on multiphoton and avalanche ionization. These processes lead to plasma formation and energy absorption in a small region confined around the focus, causing a permanent and localized modification of the bulk material. Adjusting the processing parameters a smooth refractive index increase can be obtained and light-guiding structures are produced by translating the

substrate with respect to the laser beam. Microscopic mechanisms leading to refractive index increase are complex and include densification, structural modification, color centers formation, thermal diffusion and accumulation. They concur in different ways depending on the specific material and fabrication parameter combination, i.e. wavelength, duration and energy of the laser pulses, repetition rate, objective numerical aperture (NA) and translation speed [17].

The ultrafast laser writing approach has several advantages: i) it is a maskless technique, thus particularly suited for rapid prototyping of devices; ii) it can easily fabricate buried optical waveguides in a single step; iii) it can produce optical circuits with three-dimensional layouts; iv) it can provide waveguides with a circular transverse profile [18], that can support the propagation of Gaussian modes with any polarization state, with very low waveguide form birefringence. Ultrafast laser written (ULW) waveguides in fused silica substrate have been recently employed for quantum optics experiments, still with path-encoded qubits [19]. However, it is known that ULW waveguides in fused silica are affected by material birefringence [20] (in particular when high refractive index changes are required, as in the case of curved waveguides) due to the formation of self-aligned nanogratings in the material during the irradiation process [21]. Moreover fabricating waveguides in fused silica is a rather slow process (in the order of  $10 - 100 \mu\text{m/s}$ ) [22]. For these reasons we chose to employ a borosilicate glass (EA-GLE2000, Corning) as substrate, where the formation of nanogratings has never been observed [22]. In addition, high repetition rate laser pulses induce isotropic thermal diffusion and melting of the material around the focal point [23], providing almost circular waveguide cross-section without the need for any shaping of the writing laser beam. Very low-loss waveguides are obtained with translation speeds as high as  $1\text{-}5 \text{ cm/sec}$ , allowing extremely short processing times [24]. This represents an advantage for the realization of complex photonic circuits.

At wavelengths around  $800\text{nm}$  the waveguides support a single Gaussian mode of circular profile with  $8 \mu\text{m}$  diameter at  $1/e^2$  (see the near-field intensity profile of the guided modes in the lower inset of Fig. 1), allowing a 85% overlap integral with the measured mode of the fiber used (Thorlabs SM800-5.6-125) and leading to  $0.7 \text{ dB}$  estimated coupling losses. Measured propagation losses are  $0.5\text{dB/cm}$  and using a curvature radius of  $30\text{mm}$  additional bending losses are lower than  $0.3\text{dB/cm}$ . The birefringence of the ULW waveguides has also been characterized [24], providing a value  $B = 7 \times 10^{-5}$ , thus about one order of magnitude lower than silica-on-silicon waveguides.

Ultrafast laser written beam splitters (ULWBS) were fabricated with the directional coupler geometry, as shown in Fig. 1. Straight segments and circular arcs of

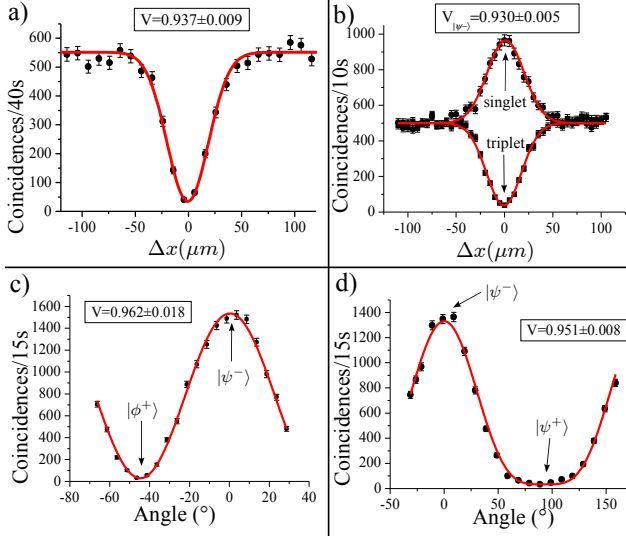


FIG. 3: a) HOM dip with input state  $|HH\rangle$ . b) peak/dip corresponding to the singlet/triplet input state. c) Fringe pattern obtained by rotating the HWP on mode  $k_B$ . d) Fringe pattern obtained by rotating the QWP on mode  $k_A$ . All curves represent experimental fits.

30mm radius were employed for an overall device length of 24 mm. Waveguides starts with a relative distance of  $250\mu\text{m}$  and in the interaction region they get as close as  $7\mu\text{m}$  (see upper inset in Fig. 1). This distance is the smallest one avoiding overlap between the two waveguides. This choice was made to minimize the sensitivity to fabrication imperfections and to obtain the shortest possible interaction length, given that future quantum optic devices will require several cascaded components integrated in the same chip. In order to optimize the length  $L$  of the central straight segments several directional couplers have been fabricated varying such length ( $L = 0 \div 1000\mu\text{m}$ ) and the corresponding splitting ratios were measured.  $L = 0\mu\text{m}$  is the shortest length yielding a splitting ratio of about 50% (see the ULWBS output modes in the lower inset in Fig. 1) at 806nm wavelength. Indeed, the possibility of achieving a 50% splitting with no straight segments is due to the coupling between the modes already occurring in the curved parts of the two approaching/departing waveguides. The reflectivity of the ULWBS for the horizontal and vertical polarizations was measured with a tunable laser operating at 806nm. The measured unbalancement between the two reflectivities  $R_H = (49.2 \pm 0.2)\%$  and  $R_V = (58.1 \pm 0.2)\%$ , is attributed to a residual ellipticity in the waveguide profile, notwithstanding the thermal mechanism of the waveguide formation. Work is in progress to further optimize the waveguide cross-section with the astigmatic beam shaping technique [18].

We demonstrated the ability of the chip to preserve any incoming polarization state by measuring the polarization degree ( $G$ ) and obtaining  $G \geq 99.8\%$ .

The suitability of the ULWBS to handle polarization encoded qubits was demonstrated by manipulating polarization entangled states. The four Bell states  $|\psi^\pm\rangle = \frac{1}{\sqrt{2}}(|H\rangle_A|V\rangle_B \pm |V\rangle_A|H\rangle_B)$ ,  $|\phi^\pm\rangle = \frac{1}{\sqrt{2}}(|H\rangle_A|H\rangle_B \pm |V\rangle_A|V\rangle_B)$  represent an entangled basis for the four dimensional Hilbert space describing the polarization of two photons. They can be grouped into the singlet state  $|\psi^-\rangle$ , generating the antisymmetric subspace, and the triplet states,  $\{|\psi^+\rangle, |\phi^+\rangle, |\phi^-\rangle\}$ , that generate the symmetric subspace, where the symmetry is referred to the exchange of the two photons [25]. The beam splitter can be used to discriminate between the symmetric and antisymmetric subspaces. Indeed if two photons in the singlet state  $|\psi^-\rangle$  impinge simultaneously on a 50/50 BS, they will always emerge on different outputs of the BS due to quantum interference. Conversely, for any state orthogonal to  $|\psi^-\rangle$  (thus belonging to the symmetric subspace) the two photons will be found in the same output mode.

The setup adopted in the experiment is shown in Fig. 2. To observe the appearance of the bosonic coalescence for input symmetric states, we varied the relative delay between the two photons and hence their corresponding temporal superposition on the ULWBS [26]. We first tested the Hong-Ou-Mandel (HOM) [26] effect with separable states, by placing two PBS in the  $k_A$  and  $k_B$  modes (see Fig. 2). We report in Figure 3a) the coincidence counts as a function of the slit delay  $\Delta x$  for two photons in the input state  $|HH\rangle$ . The measured visibility, defined as  $V_{exp} = |\frac{C_0 - C_{int}}{C_0}|$ , where  $C_0$  and  $C_{int}$  correspond respectively to the coincidence rate outside interference (i.e. with  $\Delta x$  larger than the photon coherence length) and inside interference ( $\Delta x = 0$ ). The measured visibility is  $V = 0.937 \pm 0.009$ . We performed the same measurement with the input states  $|VV\rangle$  and  $|++\rangle$  obtaining  $V = 0.926 \pm 0.012$  and  $V = 0.954 \pm 0.011$  respectively. We also tested the interference with entangled states. When the photons arrive simultaneously on the ULWBS ( $\Delta x = 0$  in the figure) we measured for the triplet (singlet) a dip (peak) in the coincidence counts as expected (see Figure 3b)). The measured visibility are  $V_{|singlet\rangle} = 0.930 \pm 0.005$  and  $V_{|triplet\rangle} = 0.929 \pm 0.005$ . We attribute the slight discrepancy observed between the theoretical<sup>1</sup> and experimental values to a partial spectral distinguishability between the photons on modes  $k_A$  and  $k_B$ : this could be reduced by using narrower bandwidth detection filters.

Let's now analyze the behavior of the different entangled states. The temporal delay was set at  $\Delta x = 0$

<sup>1</sup> Since our BS has different transmission ( $T$ ) and reflection ( $R$ ) coefficients for the  $H$  and  $V$  polarization, the maximum expected visibilities are  $V_\psi = 2\frac{\sqrt{T_H T_V R_H R_V}}{T_H T_V + R_H R_V} \simeq 0.989$  for  $|\psi^\pm\rangle$  and  $V_\phi = 2\frac{T_H R_H + T_V R_V}{T_H^2 + R_H^2 + T_V^2 + R_V^2} \simeq 0.974$  for  $|\phi^\pm\rangle$



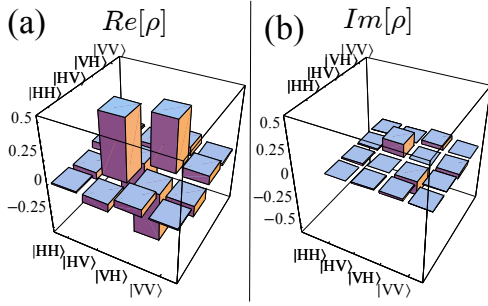


FIG. 4: Quantum state tomography of a filtered singlet state on the two output mode  $k_C$  and  $k_D$ . Real (a) and imaginary (b) part of the experimental density matrix of the filtered state.

and the source was tuned to generate the entangled state  $|\psi^+\rangle$ . By inserting on mode  $k_B$  a half waveplate (HWP) with the optical axis oriented at an angle  $\theta$  with respect to the vertical direction, the following states are generated:  $-\cos 2\theta|\psi^-\rangle + \sin 2\theta|\psi^+\rangle$ . In this case, the expected coincidence rates between detectors  $D_C$  and  $D_D$  after the beam splitter is  $\mathcal{N}_0[1 + \tilde{V} \cos 4\theta]$  where the expected visibility with the given  $R_H$  and  $R_V$  can be found to be  $\tilde{V} = 0.973$ . The experimental results are shown in Fig. 3c), yielding a visibility  $V = 0.962 \pm 0.018$ .

When the source is tuned to generate the entangled state  $|\psi^i\rangle = \frac{1}{\sqrt{2}}(|H\rangle_A|V\rangle_B - i|V\rangle_A|H\rangle_B)$ , by using a quarter waveplate (QWP) rotated at  $\theta'$  on mode  $k_A$ , the state is found to be  $\cos^2 \theta'|\psi^-\rangle - i \sin^2 \theta'|\psi^+\rangle + \frac{e^{-i\frac{\pi}{4}}}{\sqrt{2}} \sin 2\theta'|\phi^i\rangle$  with  $|\phi^i\rangle = \frac{1}{\sqrt{2}}(|HH\rangle + i|VV\rangle)$ . For the sake of simplicity, by assuming polarization independent reflectivity, the coincidence rates expected with a beam splitter with reflectivity  $R$  is  $\mathcal{N}_0[1 - V_{teo} + 2V_{teo} \cos^4 \theta']$  where  $V_{teo} = 2(1 - R)R/(2R^2 - 2R + 1)$ . By taking  $R = (R_H + R_V)/2$  we will expect  $V_{teo} = 0.987$ . The theoretical behavior was verified in the experiment. The corresponding fringe pattern, with visibility  $V = 0.951 \pm 0.008$ , is shown in Fig. 3d). These results demonstrate the high overlap between the interfering modes  $k_A$  and  $k_B$  and show that ULWBS may be used as an appropriate tool for the manipulation of polarization encoded qubit.

As a final experimental characterization we adopted the ULWBS to carry out the projection on the singlet subspace. We injected into the ULWBS the separable state  $|H\rangle_A \otimes |V\rangle_B$  and analyzed the output state when two photons emerge on the two modes  $k_C$  and  $k_D$ : the expected state reads  $|\psi^-\rangle_{CD}$ . We performed the quantum state tomography [27] of the output state conditioned to the detection of the two photons in different outputs. In this case two standard polarization analysis setup were adopted after the ULWBS (see dashed box in Fig. 2). The experimental density matrix,  $\rho_{CD}$ , shown in Figure 4 exhibits a low entropy ( $S_L = 0.071 \pm 0.018$ ), a high concurrence ( $C = 0.941 \pm 0.015$ ) and a high fidelity with the singlet state ( $F = 0.929 \pm 0.007$ ). We observe that

the present scheme achieves *a-posteriori* singlet component filtration, i.e., conditioned to the detection of one photon per output mode. Recently, a heralded entanglement filter, based on two auxiliary photons and an interferometric scheme, has been reported by adopting a bulk optical scheme in Ref. [28].

In summary, we reported on the realization and quantum optical characterization of a femtosecond-laser-written directional coupler, acting as an integrated beam splitter. The experimental results demonstrate the suitability of this method to manipulate qubit encoded in the polarization of photon states. In order to achieve a complete handling of the polarization degree of freedom the next step will consist in the realization of integrated tunable waveplates and polarizing beam splitters. By combining these tools with integrated sources of photon pairs and, possibly, with integrated detectors, the realization of pocket quantum optics lab, available for optical quantum sensing, computing and metrology may become a reality in the near future.

This work was supported by FARI project and Finanziamento Ateneo 2009 of Sapienza Università di Roma and Finanziamento Ateneo 2009 of Politecnico di Milano.

- 
- [1] N. Gisin, *et al.*, Rev. Mod. Phys. **74**, 145 (2002).
  - [2] L.-M. Duan, *et al.*, Nature **414**, 413 (2001).
  - [3] T. D. Ladd, *et al.*, Nature **464**, 45 (2010).
  - [4] P. Kok, *et al.*, Rev. Mod. Phys. **79**, 135 (2007).
  - [5] J. Dowling, Contemporary Physics **49**, 125 (2008).
  - [6] A. Politi, *et al.*, Science **320**, 646 (2008).
  - [7] A. Politi, J. C. F. Matthews, and J. L. O'Brien, Science **325**, 1221 (2009).
  - [8] J. Matthews, *et al.*, Nat. Photonics **3**, 346 (2009).
  - [9] B. J. Smith, *et al.*, Optics Express **17**, 13516 (2009).
  - [10] R. Krischek, *et al.*, Nat. Photonics **4**, 170 (2010).
  - [11] P. Walther, *et al.*, Nature (London) **434**, 169 (2005).
  - [12] M. Kawachi, Opt. Quantum Electron. **22**, 391 (1990).
  - [13] D. Jochen, *et al.*, J. Lightwave Technol. **18**, 185 (2000).
  - [14] Y. Inoue, *et al.*, J. Lightwave Technol. **15**, 1947 (1997).
  - [15] R.R. Gattass and E. Mazur, Nat. Photonics **2**, 219 (2008).
  - [16] G. Della Valle, R. Osellame, and P. Laporta, Journal of Optics A **11**, 013001 (2009).
  - [17] R. Osellame, *et al.*, Selected Topics in Quantum Electronics, IEEE Journal of **12**, 277 (2006), ISSN 1077-260X.
  - [18] R. Osellame, *et al.*, Journal of Optical Society of America B **20**, 1559 (2003).
  - [19] G. D. Marshall, *et al.*, Optics Express **17**, 12546 (2009).
  - [20] G. Cheng, *et al.*, Opt. Express **17**, 9515–9525 (2009).
  - [21] Y. Shimotsuma, *et al.*, Phys. Rev. Lett. **24**, 247405 (2003).
  - [22] M. Ams, *et al.*, Selected Topics in Quantum Electronics, IEEE Journal of **14**, 1370 (2008).
  - [23] S. M. Eaton, *et al.*, Opt. Express **16**, 9443 (2008).
  - [24] See supplementary material for details.
  - [25] K. Mattle, *et al.*, Phys. Rev. Lett. **76**, 4656 (1996).
  - [26] C. K. Hong, Z. Y. Ou, and L. Mandel, Phys. Rev. Lett. **59**, 2044 (1987).

- [27] D. F. V. James, *et al.*, Phys. Rev. A **64**, 052312 (2001).
- [28] R. Okamoto, *et al.*, Science **323**, 483 (2009).

# Supplementary informations: Polarization entangled state measurement on a chip

Linda Sansoni,<sup>1</sup> Fabio Sciarrino,<sup>1,2</sup> Giuseppe Vallone,<sup>3,1</sup> Paolo Mataloni,<sup>1,2</sup>  
Andrea Crespi,<sup>4,5</sup> Roberta Ramponi,<sup>4,5</sup> and Roberto Osellame<sup>4,5</sup>

<sup>1</sup>*Dipartimento di Fisica, Sapienza Università di Roma, I-00185 Roma, Italy*

<sup>2</sup>*Istituto Nazionale di Ottica, Consiglio Nazionale delle Ricerche (INO-CNR), L.go E. Fermi 6, I-50125 Firenze, Italy*

<sup>3</sup>*Museo Storico della Fisica e Centro Studi e Ricerche Enrico Fermi,  
Via Panisperna 89/A, Compendio del Viminale, I-00184 Roma, Italy*

<sup>4</sup>*Istituto di Fotonica e Nanotecnologie, Consiglio Nazionale delle  
Ricerche (IFN-CNR), Piazza L. da Vinci, 32, I-20133 Milano, Italy*

<sup>5</sup>*Dipartimento di Fisica, Politecnico di Milano, Piazza L. da Vinci, 32, I-20133 Milano, Italy*

## DEVICE FABRICATION

In our waveguide writing setup we employed a Yb:KYW cavity-dumped mode-locked oscillator [1], delivering 300fs, 1μJ pulses at 1030nm wavelength, with 1MHz repetition rate. Laser pulses of 240nJ were focused into the EAGLE2000 (Corning Inc.) substrate using a 0.6 NA microscope objective. Sample translation at a constant writing speed of 40mm/s was enabled by high precision three-axes air bearing stages (Aerotech Fiber-Glide 3D).

ULWBS devices were fabricated directly buried inside the glass substrate at a constant depth of 170μm.

Permanent fiber coupling of the ULWBS was obtained by gluing two pairs of fibers at the input and at the output ports and this introduced additional coupling losses lower than 0.6 dB/facet. Each pair of fibers was first inserted into a quartz double-ferrule (Friedrich & Dimmock, inc. - NJ U.S.A.), which allows to maintain a fixed distance of 250μm between the two fibers.

## WAVEGUIDE BIREFRINGENCE CHARACTERIZATION

The birefringence of the fabricated waveguides was characterized by the setup shown in Fig. 1. Six different polarization eigenstates ( $|H\rangle, |V\rangle, |+\rangle, |-\rangle, |L\rangle, |R\rangle$ ) were launched into the waveguide. The eigenstates were selected by rotating HWP1 and, if necessary, by adding also QWP1. For each of them the projections of the output state on all the same six eigenstates were measured (acting with waveplates HWP2 and QWP2), thus allowing the calculation of the normalized Stokes vectors for the output state.

It was assumed as hypothesis that the waveguide is analogous to a uniaxial birefringent material with the optical axis tilted by an angle  $\theta$ , which introduces a dephasing  $\delta$  between the two polarizations corresponding to the ordinary and extraordinary refractive index. As a conse-

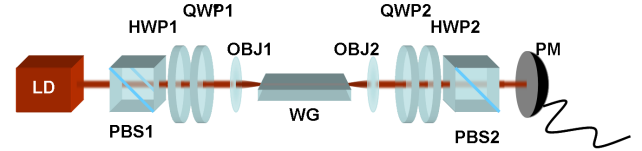


FIG. 1: Setup for birefringence measurement. LD: laser diode emitting at 806nm wavelength and with bandwidth  $\Delta\lambda = 2$  nm. PBS1 and PBS2: polarizing beam splitters. HWP1 and HWP2: half-wave plates. QWP1 and QWP2: quarter-wave plates. OBJ1 and OBJ2: objectives for injecting light into the waveguide (WG) and collecting transmitted light at the output. PM: power meter (PM).

quence, a normalized Mueller matrix of the form:

$$\begin{bmatrix} 1 & 0 & 0 & 0 \\ 0 & \cos^2 2\theta + \sin^2 2\theta \cos \delta & \sin 2\theta \cos 2\theta (1 - \cos \delta) & -\sin 2\theta \sin \delta \\ 0 & \sin 2\theta \cos 2\theta (1 - \cos \delta) & \sin^2 2\theta + \cos^2 2\theta \cos \delta & \cos 2\theta \sin \delta \\ 0 & \sin 2\theta \sin \delta & -\cos 2\theta \sin \delta & \cos \delta \end{bmatrix}$$

was fitted to the experimental data in order to determine the transfer function from the input to the output Stokes vectors.  $\delta$  and  $\theta$  were the free parameters in the fitting process.

However, a single measurement of  $\delta$  cannot be used for direct determination of birefringence, since ambiguity occurs with multiple-order birefringence. Thus, the sample was cut to different lengths and  $\delta$  and  $\theta$  were measured as described above for each length. This allowed to remove the ambiguity and yielded the actual waveguide birefringence.

In the ULW waveguides used for the experiments we found a fast axis aligned with the TE polarization and a birefringence value  $B = n_{eff, TM} - n_{eff, TE} = 7 \times 10^{-5}$ .

## SOURCE

Polarization entangled photon pairs were generated via spontaneous parametric down conversion in a 1.5mm  $\beta$ -barium borate (BBO) crystal cut for type-II non-collinear

phase matching [2], pumped by a CW laser diode with power  $P = 50\text{mW}$  and low coherence time ( $\tau_p < 1\text{ps}$ ). Degenerate photons at wavelength  $\lambda = 806\text{nm}$  were detected within a spectral bandwidth  $\Delta\lambda = 6\text{nm}$ , as determined by the interference filters. Waveplates and polarizing beam splitter (PBS) were optionally inserted in path  $k_A$  and  $k_B$  to prepare different input states. The setup shown in the dashed box have been only inserted in the quantum state tomography of the filtered state. Suitable BBO crystal compensators (C) and polarization controllers (PC) were respectively used on each photon path to compensate temporal walk-off and ensure polarization maintenance of the photons on the ULWBS. We could measure a coincidence rate  $C_{source} = 3\text{kHz}$  when photon radiation was coupled into two single mode fibers and directly connected to detectors. A delay line  $\Delta x$  in the  $k_A$  arm enabled temporal delay variation between the two input photons.

### DATA ANALYSIS

The data shown in Figure 4 were obtained by adding the measurement device shown in the dashed box placed

on the right of Figure 2, as explained in the manuscript. The additional optical component (HWP, QWP and PBS) and a more critical polarization compensation are mainly responsible of the measured fidelity of the reconstructed state. Let's try to evaluate all the imperfection contribution. We may attribute the 7% missing fidelity to the following:  $\sim 3\%$  are due to the imperfection in the source and integrated chip (a fidelity of 97% would be compatible with the average visibility reported in Figure 3),  $\sim 2\%$  of missing fidelity is due to a non perfect polarization compensation (in fact, the phase between the states  $|HV\rangle$  and  $|VH\rangle$  of the reconstructed state has a residual imaginary component as shown in Figure 4) and  $\sim 2\%$  may be attributed to the tomographic measurement setup.

- 
- [1] R. Osellame, *et al.*, Selected Topics in Quantum Electronics, IEEE Journal of **12**, 277 (2006), ISSN 1077-260X.
  - [2] P. G. Kwiat, *et al.*, Phys. Rev. Lett. **75**, 4337 (1995).